Int. J. Solids Structures Vol. 21, No. 2, pp. 161–176, 1985
Printed in the U.S.A.

0020–7683/85 $3.00 + .00

SMOOTH INDENTATION OF AN INITIALLY STRESSED ORTHOTROPIC BEAM

C. T. SUN AND B. V. SANKAR
School of Aeronautics and Astronautics, Purdue University, West Lafayette, IN 47907, U.S.A.

(*Received* 29 *July* 1983; *in revised form* 23 *April* 1984)

Abstract—The contact behavior between a smooth rigid cylinder and a simply supported orthotropic beam under uniaxial initial stresses is studied. The displacements are computed by superposing Mindlin plate solution with the solution obtained from Biot's theory of incremental deformation. Finite Fourier transforms are used in solving the equations. A point matching technique is used to compute the contact stresses and the amount of indentation for a given contact length. The effects of orthotropy and initial stresses on the contact stress distribution are investigated. An indentation law is established from the numerical results.

NOTATION

a_n	Fourier coefficients
$b_1, \ldots, b_4, d_1, \ldots, d_4$	elasticity solution constants
B_{ij}	incremental stiffness coefficients
c	semi contact length
C_{ij}	elastic constants of the orthotropic medium
E_1, E_3	Young's moduli
G_{13}	Shear modulus
h	beam thickness
i	square root of -1
k	transverse shear correction factor
k^*	dimensionless contact coefficient
L	half length of beam
n	transform variable
N_x^0	initial stress resultant
$p(x)$	load distribution
P	total load
q	exponent in indentation law
q_j	magnitude of jth pressure distribution
R	radius of indenter
S_0	magnitude of initial stress in the x-direction
s_{ij}	incremental stress components in Biot's theory
u	horizontal displacement
w	vertical displacement
w_0	vertical displacement at the center
w_{jk}	vertical displacement of jth point due to kth load distribution of unit magnitude
x, z	horizontal and vertical coordinate axes
α	indentation
γ_{ij}	incremental shear strain
ϵ_x, ϵ_z	incremental normal strains
Θ	slope of deflection curve at the supports (calculated from beam theory)
λ_1, λ_3	principal elongations due to initial stresses
ν_{13}, ν_{31}	Poisson's ratios
ξ	transform variable ($= n\pi/L$)
$\rho_1, \ldots, \rho_4$	roots of the characteristic equation
σ_x, σ_z	incremental normal stresses
τ_{xz}	incremental shear stress
ψ	beam rotation in the xz plane
ω	local rotation of a material element

1. INTRODUCTION

The problem of smooth indentation of an isotropic beam by a rigid cylinder was studied by Keer and Miller [1]. Their method superposes an infinite layer solution derived through the use of integral transforms with a pure bending beam theory solution. The problem is reduced to a Fredholm integral equation of second kind, which is solved numerically. Keer and Ballarini [2] used a similar method as above to solve the problem of contact between a rigid indenter and an initially stressed orthotropic beam. The

indentation. Moreover, an impacted structure may be under a state of initial stresses during foreign object impact, e.g. composite facing of a sandwich beam under bending loads, jet engine fan blades subjected to centrifugal forces. In such situations the methods of analysis presented here will be very useful. It is shown that the Young's modulus in the transverse direction and also the initial stresses in the beam can significantly alter the local contact behavior.

2. AUXILIARY PROBLEM

The problem to be discussed in this section is depicted in Fig. 1. The beam material is assumed to be orthotropic with the material axes of symmetry parallel to the coordinate axes. The width of the beam (in the y-direction) is assumed to be unity. Uniform initial stresses of magnitude S_0 are assumed to be present in the x-direction. Also, the beam is supposed to be simply supported. The case of clamped ends can be treated in an analogous manner. The load $p(x)$ is arbitrary, but assumed to be symmetrical about the center of the beam. The function $p(x)$ can be expressed in the form of a complex Fourier series in the interval $-L$ to $+L$. Thus,

$$p(x) = \frac{P}{2L} + \sum_{\substack{n=-\infty \\ n\neq 0}}^{\infty} a_n e^{in\pi x/L} \tag{1}$$

where P is the total load given by

$$P = \int_{-c}^{+c} p(x)\,dx$$

and a_n are the Fourier coefficients expressed by the formula

$$a_n = \frac{1}{2L}\int_{-L}^{+L} p(x)e^{-in\pi x/L}\,dx. \tag{2}$$

Actually, the load $p(x)$ can be considered as the sum of two types of loadings, namely, an U.D.L. of intensity $P/2L$ and a varying part $p_1(x)$. Thus eqn (1) may be written as

$$p(x) = \frac{p}{2L} + p_1(x). \tag{3}$$

The methods of finding the displacements due to each part of the applied load are discussed below.

2.1. *Deflection due to* U.D.L.

We assume a state of plane-strain parallel to the x-z plane. The constitutive relations

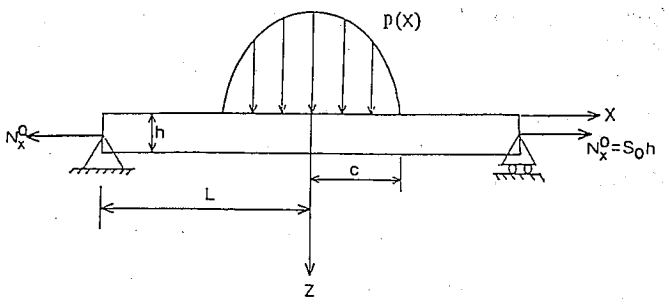

Fig. 1. Orthotropic beam subjected to axial initial stresses and an arbitrary, symmetrical transverse loading.

stresses referred to axes 1, 3 which rotate locally with the material. The local rotation ω is given by

$$\omega = \tfrac{1}{2}(w_{,x} - u_{,z})$$

where $u(x, z)$ denotes the horizontal displacement. The incremental strains for small incremental deformations are given by

$$\epsilon_x = u_{,x}, \quad \epsilon_z = w_{,z}, \quad \gamma_{xz} = w_{,x} + u_{,z}. \tag{9}$$

Biot's theory assumes that incremental stress-strain relations are linear as given below:

$$\begin{bmatrix} s_{11} \\ s_{33} \\ s_{13} \end{bmatrix} = \begin{bmatrix} B_{11} & b_{13} & 0 \\ B_{31} & b_{33} & 0 \\ 0 & 0 & Q_3 \end{bmatrix} \begin{bmatrix} \epsilon_x \\ \epsilon_z \\ \gamma_{xz} \end{bmatrix}. \tag{10}$$

The stiffness coefficients B_{ij} are generally functions of the elastic constants of the original orthotropic medium and the initial stress S_0. The details of derivation of these coefficients are given in [4] and only the results are presented here.

Let λ_1 and λ_3 be the principal elongations in directions x and z due to the initial stress S_0. Physically this means that an unit square in the x-z plane deforms into a rectangle of dimensions λ_1 and λ_3 due to application of initial stresses. We assume that the material is linearly elastic and use the constitutive relations (4) to compute λ_1 and λ_3. The incremental elastic coefficients B_{ij} are expressed in terms of the elastic coefficients of the original orthotropic medium and the principal elongations λ_1 and λ_2 as

$$\begin{aligned} B_{11} &= \lambda_1 C_{11} \\ B_{33} &= \lambda_3 C_{33} \\ B_{31} &= S_0 + \lambda_3 C_{13} \\ B_{13} &= \lambda_3 C_{13} \\ Q_3 &= C_{55}(\lambda_1 + \lambda_3)/2. \end{aligned} \tag{11}$$

It may be noted that B_{13} is not equal to B_{31}. This is because of lack of symmetry in the initial stress state.

Using the incremental stress-strain relations (10) and the strain-displacement relations (9), equilibrium equations (8) can be reduced to the following form:

$$\begin{aligned} A_1 u_{,xx} + A_2 u_{,zz} + A_3 w_{,xz} &= 0 \\ A_4 w_{,zz} + A_5 w_{,xx} + A_3 u_{,xz} &= 0 \end{aligned} \tag{12}$$

where

$$\begin{aligned} A_1 &= B_{11} \\ A_2 &= Q_3 - S_0/2 \\ A_3 &= B_{31} + Q_3 - S_0/2 \\ A_4 &= B_{33} \\ A_5 &= Q_3 + S_0/2. \end{aligned}$$

One can note that the equations of equilibrium (12) are similar to those for an orthotropic medium without initial stresses, except that the elastic constants are modified by the presence of initial stresses.

where

$$\xi = n\pi/L.$$

The solution of the above system of ordinary differential equations consists of complementary functions involving four arbitrary constants and particular integrals as given below.

$$\begin{aligned} \bar{w}(n, z) &= \sum_{i=1}^{4} b_i e^{\rho_i \xi z} - \frac{\Theta}{L\xi^2} \cos n\pi \\ \bar{u}(n, z) &= \sum_{i=1}^{4} d_i e^{\rho_i \xi z} + \frac{i\Theta}{L\xi}\left(z - \frac{h}{2}\right) \cos n\pi \end{aligned} \tag{17}$$

where ρ_is are the roots of the characteristic equation

$$\begin{vmatrix} (A_2\rho^2 - A_1) & A_3 i\rho \\ A_3 i\rho & (A_4\rho^2 - A_5) \end{vmatrix} = 0,$$

b_is are arbitrary constants, and the constants d_i are related to b_i by

$$d_i = \frac{A_3 i\rho_i}{(A_1 - A_2\rho_i^2)} b_i.$$

To evaluate the constants b_i we make use of the boundary conditions (13). The boundary conditions are first expressed in terms of displacements by using the incremental stress-strain relations (10) and strain-displacement relations (9). Then by taking transforms and substituting for $\bar{u}$ and $\bar{w}$ from eqn (17), we obtain the following simultaneous equations in b_is:

$$\begin{aligned} \sum_{i=1}^{4} \rho_i \left(A_4 - \frac{A_3 B_{31}}{A_1 - A_2\rho_i^2}\right) b_i &= -\frac{\bar{p}_1}{\xi} \\ \sum_{i=1}^{4} \rho_i e^{\rho_i \xi h} \left(A_4 - \frac{A_3 B_{31}}{A_1 - A_2\rho_i^2}\right) b_i &= 0 \\ \sum_{i=1}^{4} \frac{A_1 + (A_3 - A_2)\rho_i^2}{A_1 - A_2\rho_i^2} b_i &= 0 \\ \sum_{i=1}^{4} e^{\rho_i \xi h} \frac{A_1 + (A_3 - A_2)\rho_i^2}{A_1 - A_2\rho_i^2} b_i &= 0. \end{aligned}$$

The above equations are solved for b_is and substituted back in eqn (17) to determine $\bar{w}(n, z)$. By taking the inverse transform we obtain

$$w(x, z) = w_0(z) + \sum_{\substack{n=-\infty \\ n\neq 0}}^{+\infty} \bar{w}(n, z) e^{in\pi x/L}.$$

It can be shown that $\bar{w}(n, z) = \bar{w}(-n, z)$ and the solution reduces to

$$w(x, z) = w_0(z) + 2 \sum_{n=1}^{\infty} \bar{w}(n, z) \cos n\pi x/L. \tag{18}$$

To evaluate the term $w_0(z)$, we make use of the boundary condition $w(L, z) = 0$. Equation (18) gives the displacements due to load $p_1(x)$. The final solution is the sum of the deflection due to U.D.L. given by eqn (7) and that given by eqn (18).

and

$$w_j = \sum_{k=1}^{m} w_{jk} q_k. \tag{21}$$

From eqns (19–21) we obtain

$$\sum_{k=1}^{m} (w_{0k} - w_{jk}) q_k = x_j^2/2R, \quad j = 1, \ldots, m. \tag{22}$$

The quantities w_{0k} and w_{jk} are displacements due to unit stress distributions over known spans and they may be computed using methods discussed in Section 2. The m simultaneous equations (22) may be solved for the m unknown qs. From the contact stress distribution other quantities of interest such as total load, vertical displacements and the amount of indentation may be computed. By varying the contact length $2c$, a whole series of load-indentation relations may be developed.

The optimum number of divisions m depends upon the contact length and also the stress gradients. For example, in the beginning of indentation, contact stress distribution is nearly elliptical. So, even a small number of divisions yield converging results. As the contact length increases, there is a peaking of stresses at the ends of the contact zone and it requires larger number of divisions to get more accurate results. In the numerical examples m was varied from 10–40 depending on the contact length. The results obtained using the point matching technique are presented in Section 4.1.

3.2. *Method of assumed stress distribution*

As will be discussed later, for small contact lengths (e.g. $c/h \leq 0.5$) the contact stress distribution may be represented by an ellipse; i.e. the stresses under the indenter are given by

$$p(x) = p_0(1 - x^2/c^2)^{1/2}. \tag{23}$$

In the above equation c is the semi contact length and p_0 is the maximum value of the stress at the center. As before, we start with a known contact length $2c$ leaving p_0 as an unknown. Then we assume a similar stress distribution with some arbitrary p_0, say p_0', and compute the vertical displacements of the points in the contact zone. The average radius of curvature of the indented surface R' may be calculated using the relation

$$R' = \frac{1}{m} \sum_{j=1}^{m} \frac{x_j^2}{2(w_0 - w_j)}$$

where m is the number of reference points over the contact length; x_j is the x-coordinate of jth reference point; w_0 is the vertical displacement of the center point; and w_j is the vertical displacement of the jth point. Generally, R' will be different from the radius of the indenter R. But, the displacements vary linearly with the load and hence the peak stress p_0 required to produce a radius R is given by

$$p_0 R = p_0' R'$$

The desired load distribution is then given by eqn (23). The vertical displacements and indentation may be calculated using the methods explained earlier.

4. RESULTS AND DISCUSSIONS

The numerical results presented in this section were obtained by using the assumed stress distribution method for $c/h \leq 0.2$ and the point matching technique for $c/h \geq$

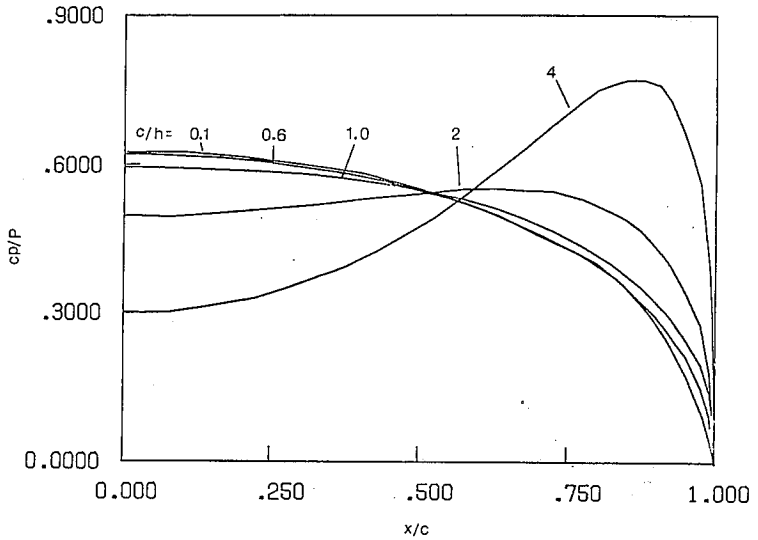

Fig. 4. Contact stresses in beam 2 ($E_3/E_1 = 1/15$).

Actually the discretized stress distributions obtained through the use of point matching technique are smoothed out in the figures. From Fig. 3 it can be seen that the nondimensionalized contact stresses are close to the results of the isotropic beam given in [3]. For small contact lengths ($c/h \leq 0.6$) the contact stress distribution is nearly elliptical. On further indentation, the stresses in the central portion of the contact zone decreases whereas there is peaking of stresses at the ends. As the beam wraps around the indenter (e.g. $c/h = 4$), the contact stresses in the central portion becomes zero. This behavior has been the discussion of [1] and [3].

From Fig. 4 it may be seen that a reduction in Young's modulus E_3 does not affect the nature of contact stress distribution at the beginning of indentation. Even for large c/h values, the deviation from the elliptical distribution is less when compared to beam 1. But opposite is the case when E_3 is increased. Figure 5 shows that in beam 3 ($E_3/E_1 = 15$) deviation from the elliptical stress distribution starts earlier and also, the peaking of stresses is more severe. The conclusion is that the local indentation behavior very much depends on E_3 whereas E_1 controls the wrapping behavior and is responsible for the peaking behavior discussed earlier.

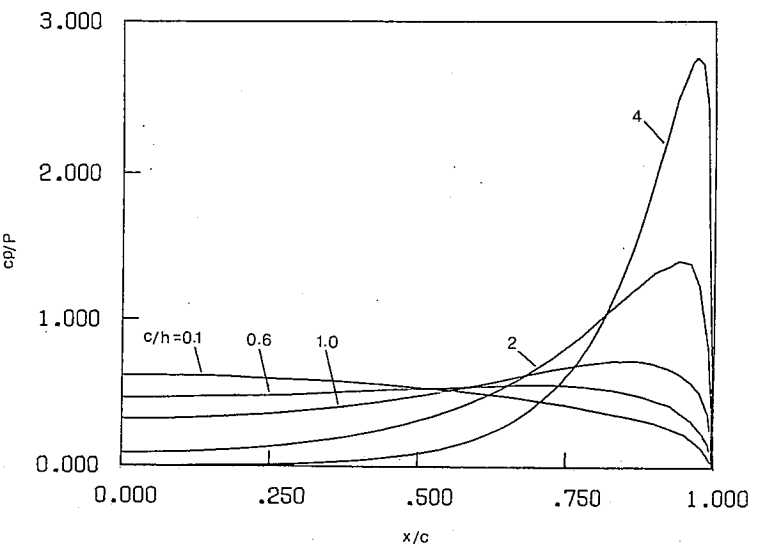

Fig. 5. Contact stresses in beam 3 ($E_3/E_1 = 15$).

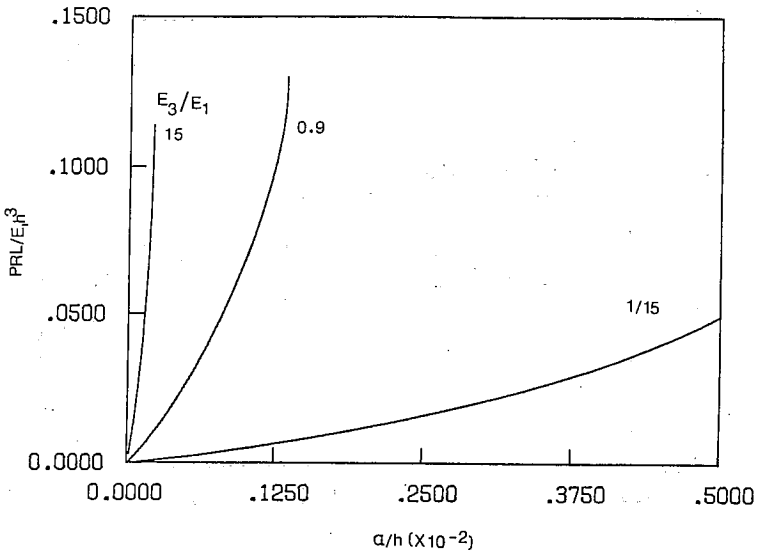

Fig. 8. Load-indentation relation (no initial stresses, α: indentation).

4.1.4. *Indentation law.* As can be seen from Fig. 8, the amount of indentation increases with the load up to a certain point and then starts decreasing with increasing load. This is due to the distribution of load over larger contact area at higher loads. It may be noted that the initial portion of the load-indentation relation, where the bending is not much in effect, may be approximated by a power law of the type

$$P^* = k^* \alpha^{*q}$$

where

$$P^* = PRL/E_1 h^3$$

$$\alpha^* = \alpha/h$$

q = exponent of the indentation law

k^* = dimensionless contact coefficient.

Least squares fitting of the data shown in Fig. 8 gives an average value of $q = 1.18$. The values of k^* are tabulated in Table 2. From this table it is obvious that the transverse Young's modulus E_3 has more effect on k^*. In general, k^* is a function of the elastic constants of the beam material and radius of the indenter. The exact functional form has not yet been found out.

4.2. *Effect of initial stresses on contact behavior*

Beam 1 which is nearly isotropic is considered in the study of the effect of initial stresses on contact behavior. The idea is to distinguish between the initial stress effect and that due to orthotropy. Both tensile and compressive initial stresses along the x-direction are considered.

Table 2. Indentation law constants for the three orthotropic materials

	Beam 1	Beam 2	Beam 3
E_3/E_1	0.9	1/15	15
k^*	215.4	17.24	1634

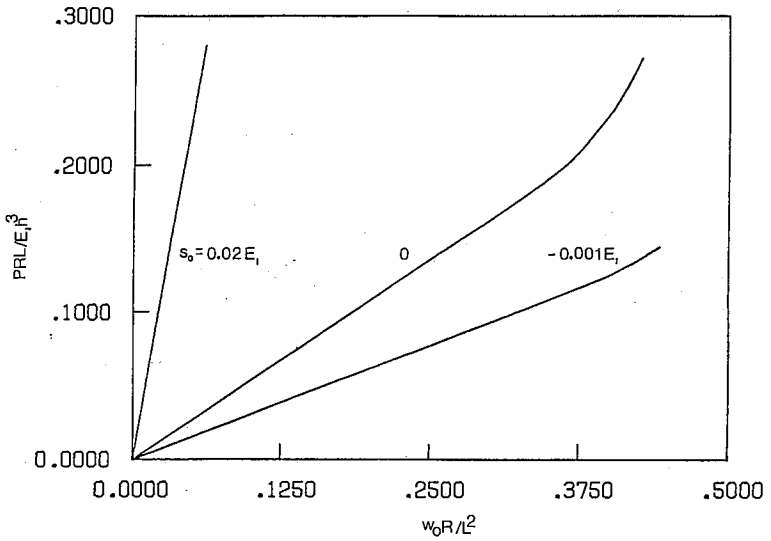

Fig. 12. Load versus indenter displacement for beam 1 under initial stresses.

4.2.1. *Contact stresses.* Figure 9 shows the stresses under the indenter for various c/h values when the beam is under initial tension. Again, for small c/h values the stress distribution is elliptical. But for higher c/h (e.g. $c/h = 4$), the stresses in the central portion of the contact area do not become zero (*cf* Fig. 3), but remain at a constant value. This contact stress is necessary to equilibrate the vertical component of the initial stresses in the bent beam. In fact, this constant value of stress is found to be nearly equal to N_x^0/R, where N_x^0 is the initial stress resultant and R is the radius of the indenter.

Curves in Fig. 10 depict the contact stress distribution when the initial stresses are compressive. At the beginning of indentation, as expected, the contact stress distribution is elliptical. But at higher contact lengths (e.g. $c/h = 4$), the contact stresses at the center become negative, implying tensile stresses. As in reality such negative contact stresses cannot exist, this suggests possible loss of contact and redistribution of contact stresses. The present analysis is not valid beyond this point and we may have to resort to a trial and error method for an exact analysis.

4.2.2. *Load-contact length relations.* Figure 11 shows the load-contact length relationship for various values of initial stresses. At the beginning of indentation, when

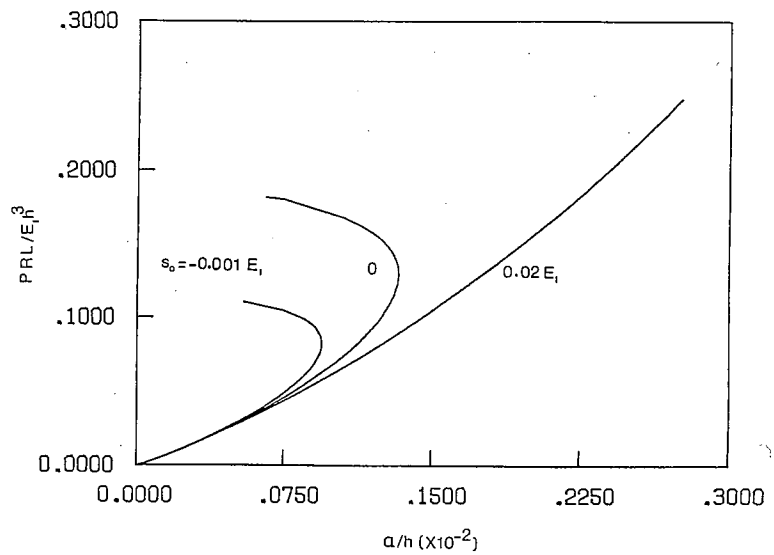

Fig. 13. Load-indentation relations for beam 1 under initial stresses.